

Filtration of Airborne Microorganisms: Modeling and Prediction

W.J. Kowalski, M.S., P.E.
Student Member ASHRAE

William P. Bahnfleth, Ph.D., P.E.
Member ASHRAE

T. S. Whittam, Ph.D.

ABSTRACT

The filtration of airborne particulates has been studied extensively and removal efficiencies can be adequately predicted from theory or from catalog data. The filtration of airborne microorganisms, however, has not been specifically addressed by theory and has seen limited empirical study. This paper addresses the variety of factors that may cause microbial filtration efficiency to deviate from predicted values based on particulate size alone. A model is developed to incorporate those factors likely to have significant impact, namely, aspect ratios and lognormal size distributions. This model is then challenged with a database of known airborne pathogens and allergens for which these parameters have been established. Results suggest existing filtration models are accurate within reason for the prediction of filtration efficiencies of airborne bacteria and spores, provided logmean diameters are used. Implications for the use of filtration in health care facilities are discussed.

INTRODUCTION

Airborne microorganisms present a challenge to engineering control of indoor air quality (IAQ) in hospital, commercial, and residential buildings. Filtration of particulates has been studied extensively, but the filtration of microorganisms remains one of the least understood applications. This paper addresses two interrelated aspects of microbial filtration necessary for accurate prediction, filter modeling and microbial modeling.

A classic mathematical model of filtration forms the basis of this methodology. This filter model incorporates multiple fiber diameters. The general mathematical models are fit to a broad range of empirical data for five grades of filters, the

HEPA 99.97% and ASHRAE 90%, 80%, 60%, and 40% filters. The HEPA is often called an absolute filter and sees applications in hospital operating rooms, TB isolation rooms, and pharmaceutical clean rooms. The other filters are all termed high-efficiency filters and are used in a wide range of hospital, health care, and commercial applications.

Microbes differ from particulate matter in several respects, such as density, the presence of hydrophobic capsules or slime layers, and in having flagella that enable motility. The factors that may cause filtration efficiency to differ from predictions based on particle size alone are reviewed.

Most microbes are spherical or ovoid and are adequately described by diameters. Some rod-like bacteria have large aspect ratios that can impact filtration efficiency. An empirical relation is used to correct the effective diameter of these microbes. Size and shape parameters for a wide array of airborne viruses, bacteria, and fungi are summarized in Table 1.

Most microorganisms occur in a range of sizes that approximate a lognormal distribution. Use of a published average value can yield inaccurate filter efficiencies. A methodology is developed that accounts for the lognormal size distribution and improves the predictive accuracy of the filter models. The results of this method are compared with efficiencies based on average diameters to demonstrate the significance of the differences.

The final set of microbial filter models are then challenged with the entire array of modeled respiratory pathogens in Table 1 to determine the most penetrating microorganisms. These proved to be predominantly nosocomial pathogens, and this result may have implications for both health care applications and for the application of filters in general.

W.J. Kowalski is a doctoral candidate and **William P. Bahnfleth** is an assistant professor in the Architectural Engineering Department, and **T. S. Whittam** is a professor in the Biology Department at Pennsylvania State University, University Park.

TABLE 1
Airborne Respiratory Pathogens—Sizes and Dimensions

AIRBORNE PATHOGEN	AVG DIA	DIA/WIDTH		LENGTH		AR	EQUIV DIA	LOGMEAN DIAMETER	LN STDEV
		MIN	MAX	MIN	MAX				
Parvovirus B19	0.022	0.018	0.026			1		0.022	0.074
Rhinovirus	0.023	0.018	0.028			1		0.022	0.088
Coxsackievirus	0.025	0.02	0.03			1		0.024	0.081
Echovirus	0.025	0.02	0.03			1		0.024	0.081
Hantavirus	0.06	0.05	0.07			1		0.059	0.067
Togavirus	0.063	0.05	0.075			1		0.061	0.081
Reovirus	0.073	0.07	0.075			1		0.072	0.014
Adenovirus	0.08	0.07	0.09			1		0.08	0.050
Orthomyxovirus	0.1	0.08	0.12			1		0.10	0.081
Coronavirus	0.11	0.08	0.13			1		0.10	0.097
Varicella-zoster	0.15	0.1	0.2			1		0.14	0.139
Arenavirus	0.18	0.05	0.3			1		0.12	0.358
Francisella tularensis	0.19	0.08	0.3	0.2	0.7	2.4	0.13	0.15	0.264
Morbillivirus	0.2	0.1	0.3			1		0.17	0.220
Respiratory Syncytial Virus	0.22	0.14	0.3			1		0.20	0.152
Parainfluenza	0.23	0.15	0.3			1		0.21	0.139
Poxvirus - Vaccinia	0.23	0.2	0.25	0.25	0.3	1.2	0.08	0.22	0.045
Mycoplasma pneumoniae	0.23	0.15	0.3			1		0.21	0.137
Paramyxovirus	0.23	0.15	0.31			1		0.22	0.145
Bordetella pertussis	0.25	0.2	0.3	0.5	1	3	0.21	0.24	0.081
Chlamydia pneumoniae	0.3	0.2	0.4			1		0.28	0.139
Chlamydia psittaci	0.3	0.2	0.4			1		0.28	0.139
Klebsiella pneumoniae	0.4	0.3	0.5			1		0.39	0.102
Haemophilus influenzae	0.43	0.2	0.3	1	1.5	5	0.43	0.35	0.081
Coxiella burnetii	0.5	0.45	0.55			1		0.50	0.040
Pseudomonas aeruginosa	0.57	0.3	0.8	1	3	3.6	0.57	0.51	0.209
Pseudomonas pseudomallei	0.57	0.3	0.8	1	3	3.6	0.57	0.51	0.209
Actinomyces israelii	0.6	0.2	1	2	5	5.8	1	0.90	0.183
Legionella pneumophila	0.6	0.3	0.9	2	2	3.3	0.57	0.72	0.091
Thermomonospora viridis	0.6	0.3	0.9	0.6	1.5	1.8	0.30	0.52	0.220
Cardiobacterium	0.63	0.5	0.75	1	3	3.2	0.57	0.65	0.107
Micropolyspora faeni	0.69	0.66	0.72			1		0.7	0.017
Thermoactinomyces sacchari	0.7	0.6	0.8	1	3	2.9	0.57	0.72	0.071
Mycobacterium kansasii	0.71	0.2	0.6	1	4	6.3	0.71	0.57	0.277
Alkaligenes	0.75	0.5	1	0.5	2.6	2.1	0.44	0.71	0.139
Yersinia pestis	0.75	0.5	1	1	2	2	0.43	0.71	0.139
Pseudomonas mallei	0.77	0.3	0.8	1.4	4	4.9	0.77	0.67	0.210
Neisseria meningitidis	0.8	0.6	1			1		0.77	0.102
Streptococcus pyogenes	0.8	0.6	1			1		0.77	0.102
Mycobacterium tuberculosis	0.86	0.2	0.6	1	5	7.5	0.86	0.64	0.322
Staphylococcus aureus	0.9	0.8	1			1		0.89	0.045
Streptococcus pneumoniae	0.9	0.8	1			1		0.89	0.045
Corynebacteria diphtheria	1	0.3	0.8	1	6	6.4	1.0	0.72	0.348
Haemophilus parainfluenzae	1	0.75	1.25			1		0.97	0.102

TABLE 1 (CONTINUED)
Airborne Respiratory Pathogens—Sizes and Dimensions

AIRBORNE PATHOGEN	AVG DIA	DIA/WIDTH		LENGTH		AR	EQUIV DIA	LOGMEAN DIAMETER	LN STDEV
		MIN	MAX	MIN	MAX				
Moraxella lacunata	1	0.8	1.2	1.5	3	2.3	0.64	0.98	0.081
Micromonospora faeni	1	0.5	1.5			1		0.87	0.220
Thermoactinomyces vulgaris	1	0.5	1.5			1		0.87	0.220
Bacillus anthracis	1.13	1	1.25			1		1.12	0.045
Nocardia asteroides	1.14	1	1.25	3	5	3.6	1.14	1.19	0.071
Mycobacterium avium	1.2	1.075	1.325			1		1.19	0.042
Mycobacterium intracellulare	1.2	1.075	0.325			1		1.2	0.042
Acinetobacter	1.25	1	1.5	1.5	2.5	1.6	0.57	1.22	0.081
Moraxella catarrhalis	1.25	1	1.5	2	3	2	0.71	1.22	0.081
Serratia marcescens	1.25	1	1.5	2	6	3.2	1.14	1.31	0.107
Nocardia brasiliensis	1.5	1	2			1		1.41	0.139
Nocardia caviae	1.5	1	2			1		1.41	0.139
Phialophora spp.	1.5	1.20	1.8	3	4	2.3	1.0	1.5	0.081
Pneumocystis carinii	2	1	3			1		1.7	0.220
Acremonium spp.	2.5	2	3	4	6	2	1.43	2.4	0.081
Geomyces pannorum	3	2	4	2	5	1.2	1.0	2.8	0.139
Histoplasma capsulatum	3	1	5			1		2.2	0.322
Paecilomyces variotii	3	2	4	3	5	1.3	1.14	2.8	0.139
Wallemia sebi	3	2.5	3.5			1		3.0	0.067
Emericella nidulans	3.25	3	3.5			1		3.2	0.031
Phoma spp.	3.25	2.5	4	6	10	2.5	2.28	3.2	0.094
Penicillium spp.	3.3	2.8	3.8	3	4	1.1	1.0	3.3	0.061
Aspergillus spp.	3.5	2.5	4.5			1		3.4	0.118
Absidia corymbifera	3.75	2.5	5			1		3.5	0.139
Coccidioides immitis	4	2	6			1		3.5	0.220
Trichoderma spp.	4.1	3.6	4.5			1		4.0	0.045
Rhizomucor pusillus	4.25	3.5	5			1		4.2	0.071
Aureobasidium pullulans	5	4	6	8	12	2	2.85	4.9	0.081
Chaetomium globosum	5.5	4.8	6.2	5.9	6.8	1.2	1.81	5.5	0.051
Cryptococcus neoformans	5.5	5	6			1		5.5	0.036
Stachybotrys spp.	5.65	5.1	6.2			1		5.6	0.039
Eurotium spp.	5.75	4.5	7			1		5.6	0.088
Scopulariopsis spp.	6	5	7	5	8	1.1	1.85	5.9	0.067
Sporothrix schenckii	6.5	5	8	10	20	2.30	4.28	6.3	0.094
Botrytis cinera	7	5	9	7	14	1.5	2.99	6.7	0.118
Mucor plumbeus	7.5	5	10			1		7.1	0.139
Rhizopus stolonifer	8	4	12			1		6.9	0.220
Cladosporium spp.	9	5	13			1		8.1	0.191
Fusarium spp.	11.5	9	14			1		11.2	0.088
Helminthosporium	12.5	7.5	8.8	27.5	60	5.4	12.47	11.6	0.156
Blastomyces dermatitidis	14	8	20			1		12.6	0.183
Rhodoturula spp.	14	12	16			1		13.9	0.058
Alternaria alternata	14.4	7	18	18	83	4	14.39	12.9	0.244
Ulocladium spp.	15	10	20			1		14.1	0.139
Paracoccidioides brasiliensis	18.25	6.5	30			1		14.0	0.306

Review Of Filtration Theory

The performance of high-efficiency ASHRAE filters is defined in terms of their total arrestance (ASHRAE 1991). Graphs of filter efficiency vs. particle size do not constitute performance requirements—they are merely a convenient way of describing performance. Filters with the same total arrestance may have different performance curves.

Figure 1 provides one set of performance curves based on laboratory measurements (Ensor et al. 1988). The arrestance of each of the four filters in Figure 1 is indicated. The efficiency at any point can fall far below or above the arrestance. Vendors generally specify arrestance as a range (i.e., 90%-95%)—the lower limit is used here as a matter of convenience. A review of various vendor catalog curves and a variety of empirical data suggest that filter performance variations of about $\pm 10\%$ are normal for any grade of high-efficiency filter.

HEPA filter performance is specified in terms of the removal efficiency at a particle size of 0.3 microns (ASHRAE 1991). Figure 2 shows the characteristic performance curve of a typical 99.97% HEPA filter with the design point indicated. This curve is merely representative of the high-efficiency filters and is not a requirement. Variations in performance occur between HEPAs from different manufacturers, but performance often exceeds requirements (Matteson and Orr 1987). Differences between HEPAs may also be reflected in terms of the most penetrating particle size or the inflection point that exists at or below the design point of 0.3 microns.

The data sets for Figure 1 and Figure 2 are among the broadest available in the literature. Though not a performance requirement, they are representative and form the basis for the filter models developed in this study.

Several mathematical models for filters exist and were tested for possible use in this analysis. Figure 3 compares the basic single-fiber models of Liu and Rubow (Raber 1986), Liu (Matteson and Orr 1987), Davies (1973), Brown (1993), and Lee and Liu (Rivers 1988) under real-world design parameters for a 90% filter. It was found, however, that none of the models gave perfect fits for all grades of filters and that all models could be adjusted to yield close fits by adjusting air velocities within the normal range (i.e., 250-800 fpm) for the respective nominal filter or by adjusting fiber diameters within normal ranges. The Rubow model (Liu and Rubow 1986) was selected for use in this analysis because of the closeness of the fit to the particular parameters shown in Figure 3 and the fact that the model's lack of an impaction component simplified the computations. Exhaustive testing showed that all of these filter models could be adapted to yield comparable predictive accuracy based on the data; therefore, this choice was essentially arbitrary.

Mathematical Model Of Filtration

The efficiency of a single fiber forms the theoretical foundation for overall filter efficiency. The single-fiber efficiency depends on particle size, air velocity, and fiber properties. The

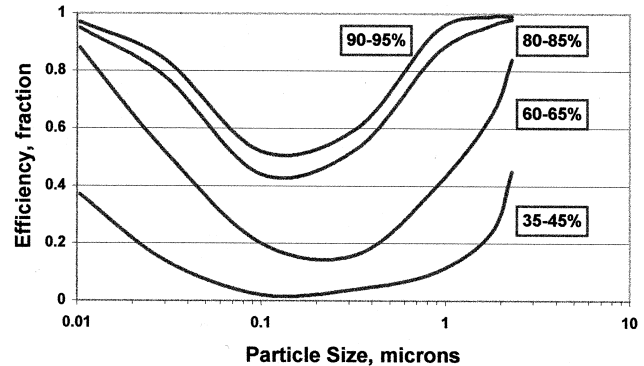


Figure 1 ASHRAE filter performance data (Ensor et al. 1988).

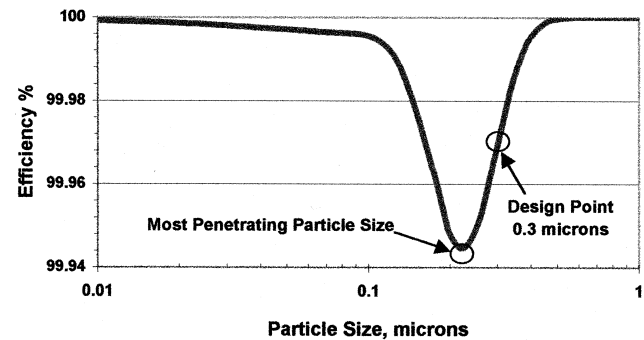


Figure 2 Typical performance of a HEPA 99.9% filter.

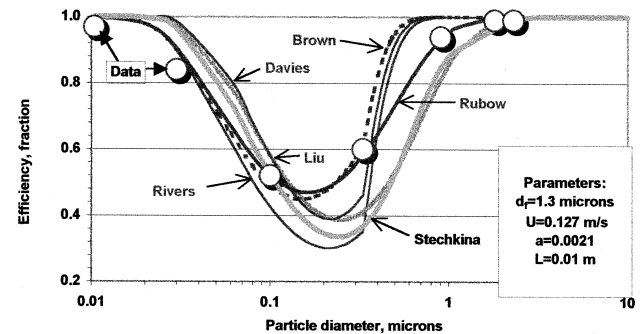


Figure 3 Comparison of various single-fiber filter models with 90% ASHRAE data from Ensor et al. (1988).

equation defining overall filter efficiency (E) for any particle size and set of conditions (Davies 1973) is as follows:

$$E = 1 - e^{-E_s S} \quad (1)$$

where

S = fiber projected area, dimensionless;

E_s = single-fiber efficiency, fractional.

The fiber projected area (S) is a dimensionless constant combining the three main determinants of filter efficiency—filter thickness (length normal to airflow), filter packing

density (packing fraction or volume fraction), and fiber diameter (Davies 1973; Brown 1993). The fiber projected area can be represented in forms that are more physically intuitive, but the mathematical definition simplifies to:

$$S = \frac{4 \times 10^6 La}{\pi d_f} \quad (2)$$

where

- L = length of filter media in direction of airflow, m;
- d_f = fiber diameter, mm;
- a = filter media volume fraction, (m^3/m^3).

Three primary mechanisms operate in filtration—impaction, interception, and diffusion. Impaction occurs when the particle inertia is so high that it breaks the air streamlines and impacts the fiber. This process is not significant for normal filter velocities and microbial sizes and is neglected in most filter models since interception satisfactorily accounts for it (Brown and Wake 1991; Brown 1993; Matteson and Orr 1987; Stafford and Ettinger 1972; VanOsdell 1994; Wake et al. 1995).

Interception occurs when a particle following a normal airflow streamline carries a particle within contact range of a fiber, at which point it will become attached by natural forces. An airstream passes through so many fibers that the probabilities are high that any particle 1 micron or larger will be intercepted in a typical high-efficiency filter.

Diffusion is a removal process that dominates for particles smaller than about 0.1 micron (Brown 1993; Davies 1973). Since these particles are subject to the effects of Brownian motion, they randomly traverse areas much wider than their diameters. This phenomenon causes attachment whether airflow streamlines bring a particle within a single diameter of a fiber or not. Lower air velocities increase the removal of small particles by diffusion since they spend more time in the vicinity of a fiber.

Figure 4 illustrates the contribution to total filter efficiency from the components of diffusion and interception. These are computed from Equation 1 as if each component

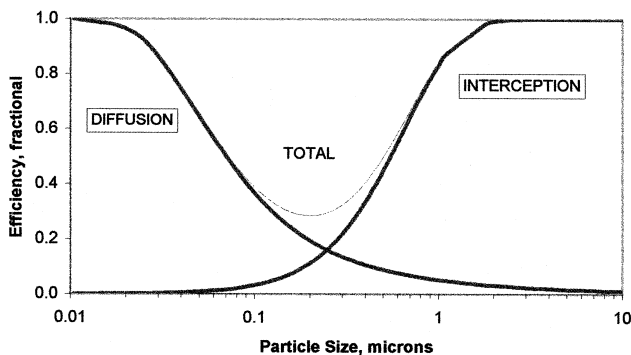


Figure 4 Generalized comparison of the contribution to total filter efficiency due to diffusion and to interception.

were a separate filter. Since interception efficiency increases with increasing particle size while diffusion efficiency decreases, a minimum occurs near where the separate efficiency curves of diffusion and interception cross. This minimum efficiency defines the most penetrating particle size.

The single-fiber efficiencies for diffusion and interception are summed to obtain the total single-fiber efficiency:

$$E_S = E_R + E_D \quad (3)$$

where

- E_R = interception efficiency, fractional;
- E_D = diffusion efficiency, fractional.

Lee and Liu (Matteson and Orr 1987) define the single-fiber diffusion efficiency as:

$$E_D = 1.6125 \left(\frac{1-a}{F_K} \right)^{\frac{1}{3}} Pe^{-\frac{2}{3}} \quad (4)$$

where

- F_K = Kuwabara hydrodynamic factor;
- Pe = Peclet number, dimensionless.

The Peclet number characterizes the intensity of diffusional deposition, and an increase in the Peclet number will decrease the single-fiber diffusion efficiency. The Peclet number is defined as:

$$Pe = \frac{1 \times 10^{-6} U d_f}{D_d} \quad (5)$$

where

- U = media face velocity (m/s);
- D_d = particle diffusion coefficient, (m^2/s).

The Kuwabara hydrodynamic factor (Liu and Rubow 1986; Brown 1993; Matteson and Orr 1987) is defined as:

$$F_K = a - (a^2 + 2lna + 3)/4 \quad (6)$$

where

- a = volume packing density, (m^3/m^3).

The particle diffusion coefficient measures the degree of diffusional motion. It is closely approximated by the same relation that defines molecular diffusion, the Einstein equation:

$$D_d = \mu k T \quad (7)$$

where

- μ = particle mobility (N-s/m);
- k = Boltzman's constant, 1.3708×10^{-23} J/K;
- T = temperature, K.

The particle mobility is defined as:

$$\mu = \frac{C_h}{3 \times 10^{-6} \pi \eta d_p} \quad (8)$$

where

- η = gas absolute viscosity, N·s/m²;
 C_h = Cunningham slip factor, dimensionless;
 d_p = particle diameter, μm .

The Cunningham slip factor accounts for the aerodynamic slip that occurs at the particle surface and is defined as:

$$C_h = 1 + \left(\frac{\lambda}{d_p}\right) (2.492 + 0.84e^{-0.435d_p/\lambda}) \quad (9)$$

where

- λ = gas molecule mean free path, 0.067 μm (Reist 1993).

Liu and Rubow (1986) defined the single-fiber interception efficiency, E_R , as:

$$E_R = \frac{1}{\varepsilon} \left(\frac{1-a}{F_K} \right) \left(\frac{N_r^2}{1+N_r} \right) \quad (10)$$

where

- N_r = interception parameter, dimensionless;
 a = volume fraction (m^3/m^3);
 F_K = Kuwabara hydrodynamic factor, dimensionless;
 ε = correction factor for inhomogeneity, dimensionless.

The interception parameter is:

$$N_r = \frac{d_p}{d_f} \quad (11)$$

In Equation 10, the correction factor $1/\varepsilon$ accounts for filter media inhomogeneity. Yeh and Liu (Raber 1986) have determined experimentally that the value of ε is approximately 1.6 for polyester filters. The same value provides acceptable agreement with empirical data for glass fiber filters as well.

Equations 1 through 11 can define the performance of any filter based on a single fiber diameter. This model can now be extended to form a multi-fiber model.

The Multi-Fiber Filtration Model

Modern high-efficiency filter media are composed of fibers of more than one diameter (Vaughan and Brown 1996). Both high-efficiency and HEPA filters consist of fiber diameters ranging from 0.65 to 6.5 microns, usually in three nominal diameter groups, according to vendor consensus.

For each nominal fiber diameter, d_i , the fiber projected area is given by Equation 12:

$$S_i = \frac{4 \times 10^6 L a_i}{\pi d_{fi}} \quad (12)$$

where

- d_{fi} = diameter of fiber i and

- a_i = volume fraction of fiber i (m^3/m^3).

The sum of the volume fractions for the fiber diameters must equal the total volume fraction. For computation purposes, each collection of discrete fiber diameters can be visualized as separate filters arranged in series. For a multi-fiber filter, the exponent in Equation 1 is the sum of the products of E_s and S for each of the discrete fiber diameters:

$$E_S S = \sum E_{si} S_i \quad (13)$$

where

- E_{si} = single-fiber efficiency for fiber i .

The single-fiber efficiency, E_{si} , is calculated individually for each fiber diameter using Equations 3 through 11 as described before, and the results are combined in Equation 13. The total efficiency is then computed with Equation 1.

Fitting The Multi-Fiber Models

Manufacturers of fibrous filter media vary the proportion of the fibers at each diameter in order to obtain the desired grade or performance. This method of proportioning fiber diameters is duplicated mathematically to fit the filter models to empirical data. The fractions a_i for each diameter are adjusted while holding all other parameters constant, including the total packing fraction a and the filter length L . For HEPA filters, however, an increase in length L is necessary to achieve the order-of-magnitude increase in efficiency.

The actual diameters of fibers and proportions at each fiber diameter are considered proprietary information by vendors and were not available. However, the absence of these data allows room for fitting the multi-fiber model to the empirical data in Figures 1 and 2. For the purposes of this analysis, the assumption is made that there are three discrete fiber diameters only—a minimum, a maximum, and an arbitrary value in between.

Table 2 summarizes the design parameters that act as constraints on filter efficiency, such as media length and filter face velocity. All of these parameters were chosen to represent typical filter design and operating parameters based on catalog data from various vendors.

Fitting of the model equations to the data was accomplished by adjusting the fiber diameters and volume fractions on spreadsheets to minimize the r^2 values in relation to the data from Ensor et al. (1988). Table 2 lists the resulting diameters, volume fractions, and the r^2 values of the fit. The resulting filter models are shown in Figure 5 along with the data points for the ASHRAE filters that were used in Figure 1.

For the 80% and 90% filters, the data points below 0.10 were neglected in the curve-fitting process to ensure an accurate fit for the data points above 0.1 microns. This recourse was taken because the filter models overpredict efficiencies at the extreme low end and the inflections inherent in the curves prevent a perfect fit. The problem lies within the model of diffusional filtration efficiency, which has seen the least focus in the literature. It would appear that the diffusional model is

TABLE 2
Multi-Fiber Filter Model Parameters

(Nominal Size: 24-by-24-in.)		HEPA 99.97%	ASHRAE High Efficiency Filters			
			90%	80%	60%	40%
Total volume fraction 'a'		0.0051	0.0020	0.0020	0.0020	0.0020
Media length, m		0.017	0.015	0.015	0.015	0.015
Face area, ft ²		3.77	3.80	3.80	3.80	3.80
Media area, ft ²		151	58	58	58	29
Nominal face velocity, FPM		250	500	500	650	750
Media velocity, FPM		6.6	34.5	34.5	44.8	103.4
Media velocity, m/s		0.034	0.175	0.175	0.228	0.526
Fiber 1	d _{f1} , microns	0.65	0.65	0.65	1.5	3.2
	fraction of total 'a'	0.5	0.16	0.1	0.1	0.01
Fiber 2	d _{f2} , microns	2.7	2.8	2.8	3.8	4.0
	fraction of total 'a'	0.35	0.5	0.5	0.4	0.1
Fiber 3	d _{f3} , microns	6.5	6.5	6.5	6.5	6.5
	fraction of total 'a'	0.15	0.34	0.4	0.5	0.89
Empirical data curve-fit r ²		NA	0.91	0.95	0.98	0.99

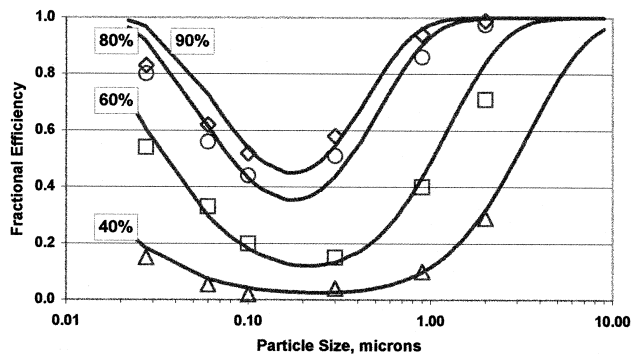


Figure 5 Comparison of filter models with ASHRAE filter data from Ensor et al. (1988).

not entirely correct in its treatment of virus particles as gaseous molecules, and this problem remains unresolved at present. This problem, which is evident in the data points to the far left of Figure 3 and Figure 5, affects the predictive validity of the model for small viruses and high-efficiency filters.

The HEPA filter model was fit to a single data point, 99.97% efficiency at 0.3 microns. However, the overprediction of diffusional efficiency, as mentioned previously, causes a deviation from empirical data which is not so insignificant in this case. To account for this, the efficiency was limited based on empirical data (Matteson and Orr 1987) for sizes below 0.2 microns. This adjustment was incorporated through the following constraint:

$$E_{max} = 0.0041d_p^2 - 0.0008d_p + 1 \quad \text{for } d_p < 0.2 \text{ microns} \quad (14)$$

Data from Sinclair (1976) also indicates HEPA performance does not reach 100% at particle sizes less than the most penetrating particle size, or about 0.1 micron. The Sinclair (1976) study used the comparatively high velocity of 0.7 m/s and found a most penetrating particle size at a lower range of about 0.03-0.05 microns.

All of the filter models compare well with available data from other sources (Whitby 1965; Thorne and Burrows 1960; Harstad and Filler 1969). The models were generally within $\pm 10\%$ of the empirical data points after adjusting to match all known study parameters such as velocity and fiber diameter.


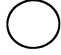

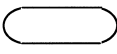



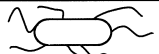


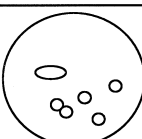
Modeling of Airborne Pathogens

Airborne microorganisms differ from particulate matter in several regards, including their individually definable sizes, shapes, size distributions, surface characteristics, and density. Modeling of these pathogen characteristics on an individual basis is necessary to ensure predictive accuracy.

The parameters for Table 1 are provided for all airborne microorganisms that can cause respiratory disease, allergies, infections, or irritation due to circulation in indoor environments, based on an extensive review of the microbiological literature (Ryan 1994; Freeman 1985; Howard and Howard 1983; Mitscherlich and Marth 1984; Burge 1989; Samson 1994). Some of these microbes have been associated with "sick building syndrome" (Godish 1995). Some of these pathogens transmit both by the airborne route and by direct contact. Fungal genera, such as *Penicillium* and *Aspergillus*, represent several species (spp).

The pathogen characteristics that are the primary determinants of filterability are size, shape, and size distribution.

TABLE 3
Shape and Aspect Ratios of Microorganisms

Shape	Type	Description	AR
	Icosahedral Helical	All respiratory viruses, whether icosahedral or helical, are so much smaller than filter fibers that they can be considered spherical for filtration calculations.	1
	Spherical	Most bacteria and spores are approximately spherical.	1
	Ovoid	Some bacteria and spores are ovoid.	1-3
	Rods	Bacteria classed as bacilli are rod-shaped.	1-10
	Diplo-cocci	Certain bacteria normally occur in pairs.	1-3
	Strepto-cocci	Some bacteria occur in strings (i.e. streptococcus) but are likely to break up on impact with filter fibers.	NA
	Staphylo-cocci	Some bacteria occur in bunches (i.e. staphylococcus) but are likely to break up on impact with filter fibers.	NA
	Flagella	Some bacteria have flagella, enabling motility.	NA
	Capsule	Some bacteria have hydrophobic capsules that can be shed or regenerated depending on the environment.	1-3
	Slime layer	Some microbes produce slime layers in addition to capsules that can be shed at any time.	1-3
	Droplets & Droplet Nuclei	Aerosolized droplets, typically 20-100 microns, may contain numerous microbes and other particles. These evaporate to condensation nuclei that may contain several viable microbes and residue. These will break up upon impact with filter fibers.	1-3

Characteristics that have a minor or potential impact on filterability are the density, adherence or surface characteristics, and motility. These characteristics are addressed individually.

Size and Shape

In Equations 1 through 14, particle size is defined in terms of a representative diameter. Since not all microbes are spherical, shape becomes a secondary determinant of size. The types of shapes that pathogens may have are identified graphically in Table 3.

Larger groups of microbes, strepto-cocci, staphylo-cocci, and droplet nuclei, are held together by very weak natural forces and are likely to break up on aerosolization or on impact with filter fibers. The end result is that microbes will be reduced to singular forms during the process of filtration. If not, for whatever reason, then they remain as larger particles and predicted filtration efficiency will be conservative.

Most microbes are spherical, ovoid, or short rods and can be effectively modeled as spheres for the purpose of filtration. Longer rods can be conveniently defined in terms of an aspect ratio (AR) or the ratio of length to width. The aspect ratio provides the basis for determining the equivalent diameter of nonspherical microbes.

For microbes with an aspect ratio of less than about 3.5, the minimum diameter or width is a conservative value to use for the effective diameter. An empirical study by Benarie (Matteson and Orr 1987) determined statistically that for particles with a large aspect ratio that arrive at the filter surface unoriented, the effective diameter, D_e , is:

$$D_e = 0.285L \quad [for Re < 2.0] \quad (15)$$

where

L = diameter, microns;

Re = Reynolds number for the particle.

The above relation was applied to the pathogens whenever $AR > 3.5$ to determine the equivalent diameter shown in Table 1. The value calculated from Equation 15 was selected for use only when it resulted in a larger equivalent diameter. The Reynolds number was based on a particle velocity of 0.66 m/s (compare with the velocities in Table 2).

Size Distribution

The distribution of the size of any microbe tends to follow a lognormal distribution curve, or a curve in which the logarithm of size is distributed normally. This is typical of bioaero-

sols and even most particulates near the micron size range (Reist 1993; Painter and Marr 1968; Duguid 1945). Studies on cell size distribution indicate the lognormal distribution of cell size predominates both during division, growth phases, and for full-grown microbes (Koch 1966, 1995; Koppes et al. 1978; Zaritsky 1975). Other mathematical expressions can be used to describe these characteristic distributions, such as Pearson curves, but the lognormal curve is adequate.

Figure 6 illustrates the theoretical size distribution of *Chlamydia pneumoniae*. The logmean diameter lies to the left of the average diameter. On a logarithmic scale, this curve has a normal distribution about the logmean diameter and is defined by a standard deviation.

The lognormal distribution can be computed based on the probability density of the normal distribution (Bliss 1967; Reist 1993) of a set of diameters:

$$Z = \frac{1}{\sigma\sqrt{2\pi}} e^{-\frac{1}{2}((y-\psi)/\sigma)^2} \quad (16)$$

where

- Z = probability density,
- σ = standard deviation of ln (diameter),
- ψ = mean of ln (diameter),
- y = ln (diameter).

The only parameters necessary to develop a lognormal distribution curve are the range of diameters, the standard deviation, and the logmean diameter. In the absence of additional distribution data, the logmean diameter is approximately equal to the average of the logarithms of the minimum and maximum diameter.

The standard deviation for lognormal size distributions of bacteria is typically from 10% to 30% of the size range, based on inspection of published data (Koppes et al. 1978; Tyson 1986; Harvey et al. 1967). A logarithmic standard deviation of 0.2 times the range is assumed for all microorganisms. The filtration efficiency is not sensitive to this range of logarithmic

standard deviations, and, therefore, this assumption is reasonable. The final column of Table 1 lists the logarithmic standard deviation (LN STDEV) for each microbe, computed as 20% of the difference between the minimum and maximum diameter.

The size distribution curve is generated by establishing ten population blocks between the minimum and maximum logarithmic diameter, as shown in Figure 6. Each block is represented by a mean and spans $\pm 5\%$ of the total range. The population fraction of each block was determined by numerically integrating Equation 16 to get the population fractions. It was found, post analysis, that no significant difference resulted from simply using the logmean diameters as opposed to performing size-distribution calculations. This is the method recommended because of its simplicity, and the logmean diameters, incorporating aspect ratios and determined by the size-distribution calculations, are provided in Table 1 for use.

The results of a size distribution calculation are illustrated graphically in Figure 6, in which the continuous probability density curve has been converted into blocks of population fractions at each of the indicated mean diameters. A similar procedure was performed to establish the population fractions (blocks) versus size for each microbe in Table 1.

Finally, each of the ten mean diameters of the size distribution will have an associated efficiency calculated by Equations 1 through 14. The overall efficiency of filtration for each microorganism is the sum of the filtration efficiencies for each mean diameter subdivision, as follows:

$$\eta_{tot} = \sum_{i=1}^{10} 0.10\eta_i \quad (17)$$

where

- η_i = filtration efficiency for each microbial population block defined by a discrete mean diameter.

Density

The smallest microbes are filtered mainly by diffusion, and, therefore, density is not a factor. The density of larger microbes can affect their filterability. Previous studies have assumed that microbes have the density of water (Miller-Leiden et al. 1996). The actual buoyant density of bacteria has been found to be 1.03-1.10 times that of water (Bakken and Olsen 1983). However, this density results in an almost negligible increase in removal efficiency due to impaction. This effect could be neglected, except perhaps in cases of high-velocity airflow through low-efficiency filters. The density of spores has not been studied, but it is likely to be very similar to that of bacteria.

Surface Characteristics

Most bacteria have a tough outer cell wall made from a tightly woven mesh of polymer-like molecules. The cell wall encloses a balloon-like inner cell containing plasma and cellular components. The internal pressure of a bacterial cell can be

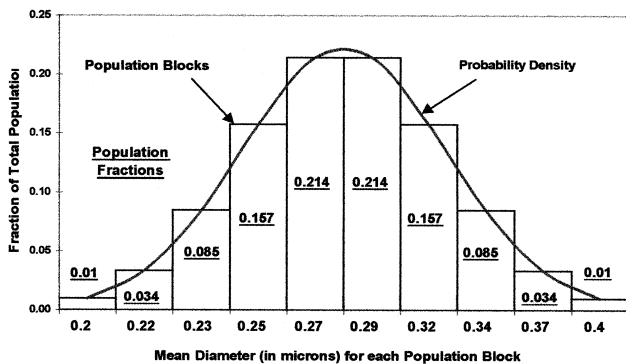


Figure 6 Lognormal distribution curve of *Chlamydia pneumoniae*. Division of population into ten blocks is shown in comparison with the continuous probability density curve (normalized).

on the order of 50-60 psia (Koch 1995; Ryan 1994), or about the pressure in a truck tire. Bacteria are, therefore, similar to solid particles except that some species may have detachable capsules or an outer surface covered with a slime layer. Such gelatinous surfaces could conceivably decrease microbial filterability.

Surface stickiness, or adherence, may affect filterability. Bacteria have a strong affinity for adherence to glass surfaces (Ellwood et al. 1979), and fiberglass filter media may already be the ideal filter material. Polyester filter media are also in use, and a comparison of their relative ability to filter airborne microbes might provide interesting conclusions on the significance of material-dependent adherence.

Most microorganisms have a negative surface charge (Ellwood et al. 1979). If this charge were significant, then a fiber with a natural positive charge would be likely to provide enhanced microbial filtration. Artificial means of inducing electrostatic charges, either on the particles or on the filter media, have been promising in theory, but empirical data indicates electrostatic efficiency improvements are marginal (Offermann et al. 1991).

Motility

A few of the bacteria in Table 1 possess flagella, which enable movement, or motility. Motile bacteria move toward chemical attractants and avoid chemical repellents (Ryan 1994). Although flagella enable motility in water, it is conceivable that motile bacteria such as TB bacilli might be able to free themselves from attachment to a filter fiber and become re-entrained in the airstream. However, numerous fiber impacts would follow, and so the only benefit of motility might be movement along fibers to areas with moisture and nutrients.

No viruses or spores are motile. Spores and some bacteria, however, will grow in the presence of moisture and so the possibility exists that microbes intercepted by a filter may, in time, be able to “grow through” the filter and become liberated into the air on the downstream side. No data currently exist to quantify the effects of motility or grow-through on microbial filtration.

Droplet Nuclei

Droplet nuclei are defined as droplets that have evaporated to form clumps of microbes and condensable matter. Theoretically, a droplet several microns in diameter should evaporate within seconds even in humid air (Reist 1993). Empirical data, however, suggest that some small fraction of micron-sized droplets can remain airborne for hours (Duguid 1945).

Since droplets and droplet nuclei are held together by surface tension or other minor forces, they will break up on impact with filter fibers and reduce to smaller constituents. The breakup of water droplets enhances evaporation, as it does in cooling towers and evaporative coolers. The end result is that most microbes contained in a droplet will be subject to

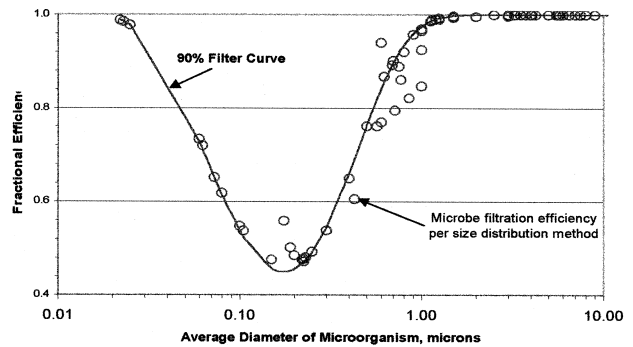


Figure 7 Deviations of predicted filter performance for a 90% filter. The circles indicate predictions of the size distribution method.

filtration at their actual diameters. Droplet nuclei that fail to break up become filtered at larger diameters, and so the predicted efficiency based on microbial diameter will always be conservative.

RESULTS AND DISCUSSION

Figure 7 illustrates the effects of using a particle size distribution model, as opposed to using a standard model based on average diameters, for an ASHRAE 90% filter. The performance curve represents predicted efficiency based on average diameters. The circles each represent the predicted filtration efficiency using the size distribution method as described previously. The x-axis location of each circle indicates the average diameter. Data for the 40%, 60%, and 80% ASHRAE filters show similar deviations, though proportionally less pronounced. In general, for sizes above 0.3 microns, the use of average diameters will overpredict filtration efficiency for particles that have a wide size distribution. However, the overpredictions are typically within 5%-15%, and since this is essentially within the range of normal variations between the performance of different filters with the same nominal efficiencies, these overpredictions are not necessarily significant.

Of the 90 airborne pathogens in Table 1, 19 demonstrate deviations of 5% or more from predictions based on using average diameters. Figure 8 summarizes these pathogens and illustrates the deviations in terms of penetration for the 40%, 60%, 80%, and 90% ASHRAE filters. Most of these microbes show increased penetration over that which would be predicted based on using average diameters. As noted previously, these differences in predicted filtration efficiency, or penetration, are mostly within the range of accuracy of the filter models and of variations between manufacturers. However, the use of the size distribution method may be justified for those microbes possessing a defined wide size distribution and where increased predictive precision is required.

The observation can be made, from Figure 7 or from calculations with the model, that even a medium-efficiency filter is capable of removing the largest portion of common spores (typically 1 micron and larger) in a single pass.

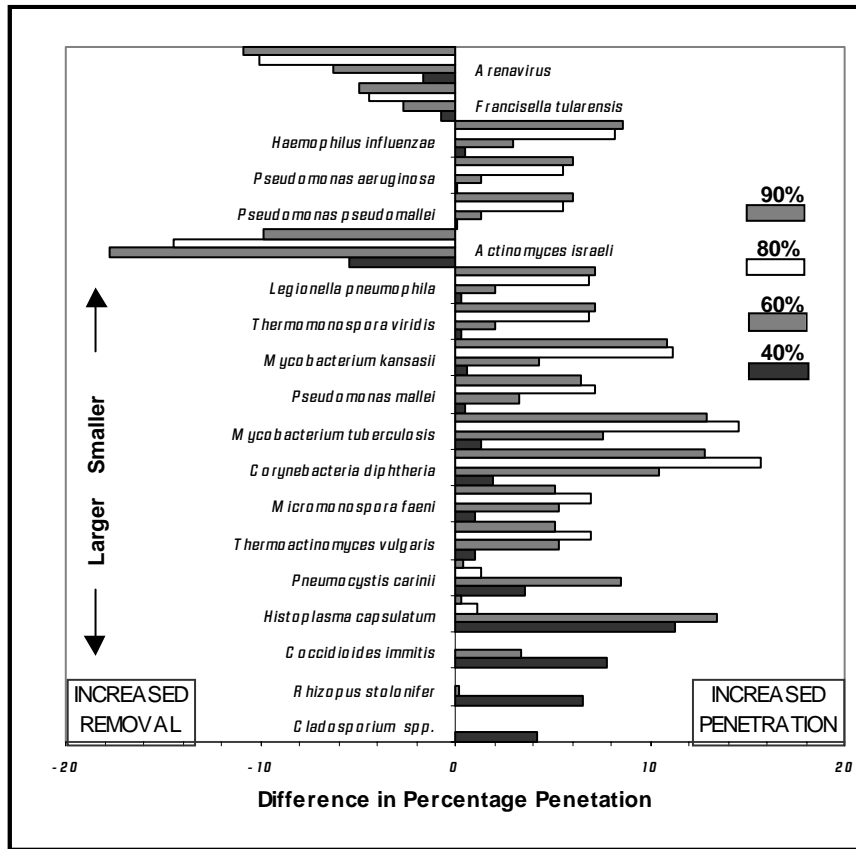


Figure 8 Difference in predicted filter penetration by the size distribution method over predictions based on average diameter.

Medium-efficiency filters in recirculation systems, even with outside air mixing, would remove spores at efficiencies that would exceed their nominal rating and rival that of HEPA filters. A similar argument can be made with regard to bacteria and high-efficiency filters. Analytical support exists here for reiterating the suggestion (Luciano 1977) that the use of HEPA filters in health care (or other) applications may represent overfiltering of airstreams. This may be especially true when UVGI systems, which are effective against viruses and many smaller bacteria, are used in combination with HEPA filtration.

As an application of the size distribution model and its enhanced predictive capabilities, HEPA filtration effectiveness has been examined to determine the most penetrating microorganisms. For a single pass through a HEPA 99.97% filter, the number of penetrations per million for each microbe in Table 1 was calculated. Figure 9 shows the results of this analysis, where only those microbes that experienced penetration above about 30 per million are listed. All of the microbes between *H. influenzae* and *Varicella* experienced penetrations greater than 1 in 10,000. This may be insignificant, especially for a single pass through the filter,

but it depends on the airborne concentration and the infective dose for each microorganism.

The infective dose for *M. tuberculosis* is 1-10 bacilli and that for *M. pneumoniae* is about 100 (Ryan 1994). Few other infective doses are known with certainty, but such data could form the groundwork for detailed analysis of the risks inherent, not only for HEPAs, but for filters in general.

An intriguing aspect of Figure 9 is that almost all of the most penetrating microorganisms are agents of nosocomial infections. HEPA filters are widely used in hospital operating rooms and isolation wards, and further study of this matter may be warranted.

The use of complete size distribution data is rather cumbersome, and an alternative method for predicting microbial filtration efficiency is to use the logmean diameters. The logmean diameters have been determined and presented for use in Table 1, and these values should be used in preference to published average microbial diameters. A simple computation of filter efficiency for any microbe using logmean diameters will give results virtually indistinguishable from using the complete size distribution method.

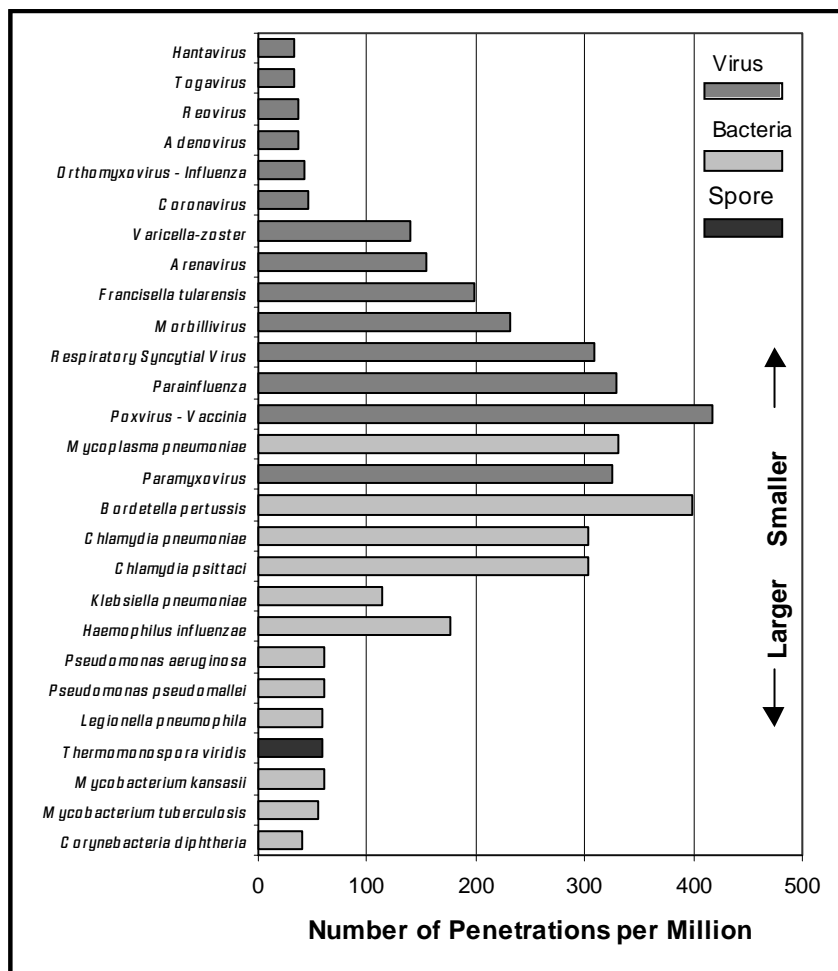


Figure 9 The most penetrating microorganisms: HEPA 99.9% filter, single pass.

CONCLUSIONS

In conclusion, the results of this analysis indicate that existing filter models are adequate for predicting the filtration efficiency of bacteria and spores provided that the logmean diameters, not the average diameters, are used for particle size. The filtration efficiencies of the smallest viruses, however, cannot be conservatively predicted due to the limitations of existing filtration theory in this size range. This matter could not be resolved and remains to be researched further.

Results suggest that the use of logmean diameters with existing filter models can improve predictive accuracy by 5% to 15% for certain microbes, although this range of improvement is essentially within the normal range of filter performance variation for any given nominal efficiency.

Results indicate that medium- to high-efficiency filters should be effective in removing such large proportions of bacteria and spores that HEPA filters may represent overfiltering, even for health care facilities. This is especially true

where filtration is used in combination with UVGI, which can be effective against viruses and many smaller bacteria, or in recirculation systems where multiple passes through the filter may occur.

One collateral finding of this analysis that may be of some interest to designers of operating rooms is that the microorganisms spanning the most penetrating particle size range of HEPA filters are predominantly nosocomial infections. The degree of penetration may not be significant but may warrant some evaluation of the risks.

ACKNOWLEDGMENTS

Thanks to ASHRAE for their kindness and foresight in supporting this research with a Grant-in-Aid. Thanks also to Don Thornburg of Farr Co., R. Vijayakumar, Tim Hudson, and Marianne Lane of Hollingsworth & Vose Company, Chuck Rose of AAF International, and Bill Cambo of Lydall, who provided technical support and consultation.

REFERENCES

- ASHRAE. 1991. *1991 ASHRAE Handbook—HVAC Applications*, Health facilities. Atlanta: American Society of Heating, Refrigerating and Air-Conditioning Engineers, Inc.
- Bakken, L.R., and R.A. Olsen 1983. Buoyant densities and dry-matter contents of microorganisms: Conversion of a measured biovolume into biomass. *Appl. & Environ. Microbiol.* 45 (4): 1188-1195.
- Bliss, C.I. 1967. *Statistics in biology*. New York: McGraw-Hill.
- Brown, R.C., and D. Wake 1991. Air filtration by interception—theory and experiment. *J. Aerosol Science* 22(2): 181-186.
- Brown, R.C. 1993. *Air filtration*. Oxford: Pergamon Press.
- Burge, H.A. 1989. Airborne allergenic fungi: Classification, nomenclature, and distribution. *Immunol. Allergy Clinics North Amer.* 9(2): 307-309.
- Davies, C.N. 1973. *Air filtration*. London: Academic Press.
- Duguid, J.P. 1945. The size and the duration of air-carriage of respiratory droplets and droplet-nuclei. *J. Hyg.* 54: 471-479.
- Ellwood, D.C., J. Melange, and P. Rupture. 1979. *Adhesion of microorganisms to surfaces*. London: Academic Press.
- Ensor, D.S., A.S. Viner, J.T. Hanley, P.A. Lawless, K. Ramanathan, M.K. Owen, T. Yamamoto, and L.E. Sparks. 1988. Air cleaner technologies for indoor air pollution. *IAQ 88, Engineering solutions to indoor air problems*. Atlanta: American Society of Heating, Refrigerating and Air-Conditioning Engineers, Inc.
- Freeman, B.A., ed. 1985. *Burrows textbook of microbiology*. Philadelphia: W.B. Saunders Co.
- Godish, T. 1995. *Sick buildings: Definition, diagnosis and mitigation*. Boca Raton: Lewis Publishers.
- Harstad, J.B., and M.E. Filler. 1969. Evaluation of air filters with submicron viral aerosols and bacterial aerosols. *Am. Indust. Hyg. Assoc. J.* 30: 280-290.
- Harvey, R.J., A.G. Marr, and P.R. Painter. 1967. Kinetics of growth of individual cells of *Escherichia coli* and *Azotobacter agilis*. *J. Bact.* 93 (2): 605-617.
- Howard, D.H., and L.F. Howard. 1983. *Fungi pathogenic for humans and animals*. New York: Marcel Dekker, Inc.
- Koch, A.L. 1966. The logarithm in biology: Mechanisms generating the lognormal distribution exactly. *J. Theoret. Biol.* 12: 276-290.
- Koch, A.L. 1995. *Bacterial growth and form*. New York: Chapman & Hall.
- Koppes, L.J.H., C.J. Woldringh, and N. Nanninga. 1978. Size variations and correlation of different cell cycle events in slow-growing *Escherichia coli*. *J. Bact.* 134: 423-433.
- Liu, B.Y.H., and K.L. Rubow. 1986. *Air filtration by fibrous media*. Fluid filtration: gas. Philadelphia: American Society for Testing and Materials.
- Luciano, J.R. 1977. *Air contamination control in hospitals*. New York: Plenum Press.
- Matteson, M.J., and C. Orr, eds. 1987. *Filtration: Principles and practices*. New York: Marcel Dekker, Inc.
- Miller-Leiden, S., C. Lobascio, and W.W. Nazaroff. 1996. Effectiveness of in-room air filtration and dilution ventilation for tuberculosis infection control. *J. Air and Waste Mgt. Assoc.* 46 (9): 869.
- Mitscherlich, E., and E.H. Marth. 1984. *Microbial survival in the environment*. Berlin: Springer-Verlag.
- Offerman, F.J., S.A. Loisel, and R.G. Sextro. 1991. Performance comparison of six different air cleaners installed in a residential forced-air ventilation system. *IAQ 91, Healthy buildings*. Atlanta: American Society of Heating, Refrigerating and Air-Conditioning Engineers, Inc.
- Painter, P.R., and A.G. Marr. 1968. Mathematics of microbial populations. *Ann. Rev. Microbiol.* 22: 519-549.
- Raber, R.R. 1986. *Fluid filtration: Gas*. Symposium on Gas and Liquid Filtration. Philadelphia: American Society for Testing and Materials.
- Reist, P.C. 1993. *Aerosol science and technology*. McGraw-Hill: New York.
- Rivers, R.D. 1988. Interpretation and use of air filter particle-size-efficiency data for general-ventilation applications. *ASHRAE Transactions* 88(2): 1835-1849.
- Ryan, K.J., ed. 1994. *Sherris medical microbiology*. Norwalk: Appleton & Lange.
- Samson, R.A., ed. 1994. *Health implications of fungi in indoor environments*. Amsterdam: Elsevier.
- Sinclair, D. 1976. Penetration of HEPA filters by submicron aerosols. *J. Aerosol Science* 7: 175-179.
- Stafford, R.G., and H.J. Ettinger. 1972. Filter efficiency as a function of particle size and velocity. *Atmospheric Environment* 6: 353-362.
- Thorne, H.V., and T.M. Burrows. 1960. Aerosol sampling methods for the virus of foot-and-mouth disease and the measurement of virus penetration through aerosol filters. *J. Hyg.* 58: 409-417.
- Tyson, J.J. 1986. Sloppy size control of the cell division cycle. *J. Theoret. Biol.*, 118: 405-426.
- Van Osdell, D.W. 1994. Evaluation of test methods for determining the effectiveness and capacity of gas-phase air filtration equipment for indoor air applications. *ASHRAE Transactions* 100(2): 511-523.
- Vaughan, N.P., and Brown, R.C. 1996. Observations of the microscopic structure of fibrous filters. *Filtration & Separation*, Sept., pp. 741-748.
- Wake, D., A.C. Redmayne, A. Thorpe, J.R. Gould, R.C. Brown, and B. Crook. 1995. Sizing and filtration of microbiological aerosols. *J. Aerosol Science* 26 (S1): s529-s530.
- Whitby, K.T. 1965. Calculation of the clean fractional efficiency of low media density filters. *ASHRAE Journal* Sept., pp. 56-65.

Zaritsky, A. 1975. On dimensional determination of rod-shaped bacteria. *J. Theoret. Biol.* 54: 243-248.

DISCUSSION

Eric Brodsky, Research Products, Madison, Wisc.: How does the size of an airborne virus compare with the measured size of a clean lab virus?

W.J. Kowalski: No significant differences should exist between the size of a virus measured by means such as electron microscopy in a laboratory and the same virus measured by an aerosol particle sizer. Each method, however, can have inherent errors and so some differences could be expected. Variations in size due to layers of bound water and the presence or absence of capsules could also be expected, but these should be accounted for by the minimum and maximum dimensions shown in Table 1.

Karin Foarde, Senior Research Microbiologist, Research Triangle Institute, Research Triangle Park, North Carolina: Are the size distributions for the microbes based on empirical data?

W.J. Kowalski: The size distributions were developed theoretically, but they are based on known minimum and maximum dimensions for each species and on coefficients of variation from a number of studies. Very few size distributions have been published, but they closely match the theoretical curves. We corroborated the size distribution for *Legionella* using a Coulter counter but these results are incomplete. Research is needed to determine the size distributions for all the major airborne pathogens, especially non-spherical microbes like *Mycobacterium tuberculosis*. Some changes to the mean diameters in Table 1 could result.